Efficient Inelastic Fiber Frame Element and Consistent Damping Model for Seismic Time-History Analyses

P. Jehel
Laboratoire MSSMat (UMR 8579), École Centrale Paris, CNRS, France
e-mail: pierre.jehel[at]ecp.fr

A. Ibrahimbegovic
LMT-Cachan (ENS Cachan/CNRS/UPMC/PRES UniverSud Paris), France

P. Léger
École Polytechnique of Montreal, Dpmt. of Civil Engineering, Canada

SUMMARY:
This paper deals with modeling reinforced concrete (RC) frame structure in seismic motion with inelastic time-history analyses. Such analyses require the definition of an inelastic structural model – that is capable of dissipating part of the imparted seismic energy – and additional damping is generally added, *e.g.* Rayleigh damping. This additional damping has to be consistent with the inelastic structural model: it has to account for energy dissipation mechanisms not otherwise explicitly modeled. A consistent damping model is presented in this paper and the simulation of a 2D RC frame tested on a shaking table is performed with this latter damping model. Results are then used as a baseline to assess the consistency of another more common Rayleigh damping model.

Keywords: Inelastic time-history analyses; Frame structures; Fiber element; Reinforced concrete; Energy dissipation; Consistent additional damping.

1. INTRODUCTION

Modeling energy dissipation in seismic inelastic time-history analyses (ITHAs) has been challenging practitioners and researchers for the last few decades. Adding damping in ITHA is common practice, *e.g.* Rayleigh damping – damping coefficients are computed as a linear combination of mass and stiffness –, yet it is well known that it can lead to inaccurate results. Regarding the continuous development of numerical inelastic structural elements, where part of the seismic energy is dissipated by explicitly modeling inelastic phenomena, added damping should only represent energy dissipative mechanisms not otherwise considered in the structural model (PEER/ATC-72-1 October 2010). In other words, the additional damping model should be consistent with the inelastic structural one.

Rayleigh damping is commonly used in ITHAs. Nevertheless, it has been shown that it is difficult to control the amount of damping it generates throughout ITHAs (Léger & Dussault 1992, Hall 2006, Charney 2008). The ultimate strategy to avoid inaccurate results due to additional damping in seismic ITHAs is to use an inelastic structural model that is capable of representing all the energy dissipative phenomena occurring during the seism. More practicable is the development of structural elements that can accommodate additional damping models, as in (Zareian & Medina 2010) where the authors develop a frame element as the combination of an elastic part with stiffness-proportional damping and two inelastic springs at its two ends with no stiffness proportional damping. It is claimed that this method eliminates the presence of unrealistic damping forces in ITHAs.

With most of the existing inelastic structural models, the consistency of Rayleigh damping has to be checked. The purpose of this paper is to propose a consistent additional damping model of the Rayleigh type, adapted to both the capability of the inelastic structural model to dissipate seismic energy and the seismic demand. Then, this damping model is used as a baseline to check the consistency of a more commonly used Rayleigh damping model in the seismic ITHA of a RC frame structure.

We first briefly present the theoretical formulation of a fiber frame element with enhanced kinematics to incorporate a 1D constitutive law (Jehel et al. 2010) developed in the framework of thermodynamics with internal variables. The resulting element accounts for the main energy dissipative phenomena encountered in concrete and steel fibers of reinforced concrete (RC) frame elements, except those coming

from steel-concrete interactions and rebar buckling. Then, in section 3, a consistent additional damping model is proposed according to the definition of three successive phases in a typical frame structural response. Finally, a 2-bay 2-storey RC moment-resisting frame structure tested on the shaking table of Ecole Polytechnique de Montréal (Filiatrault et al. 1998a) is simulated with both the proposed consistent damping model and another common Rayleigh model. The results obtained are compared to experimental data.

2. INELASTIC FIBER FRAME ELEMENT WITH ENHANCED KINEMATICS

The inelastic structural model is based on a fiber frame element suitably implemented in the framework of a displacement-based formulation so that it can integrate the uniaxial concrete behavior law recently developed by the authors (Jehel et al. 2010). This latter constitutive model is capable of representing the main energy dissipative phenomena likely to occur in concrete: appearance of permanent deformation, strain hardening and softening, stiffness degradation, local hysteresis loops, appearance of cracks. Its theoretical development and numerical implementation are based on thermodynamics with internal variables (Germain et al. 1983, Maugin 1999) and on the finite element method with embedded strong discontinuities (Garikipati & Hughes 1998, Ibrahimbegovic & Brancherie 2003, Oliver & Huespe 2004). FEAP (FEAP 2002) is the finite element program used for the numerical implementation of the developments presented in this section.

2.1. Enhanced kinematics

The first ingredient of this model is the definition of an enhanced kinematics where strong discontinuities – displacement jumps – are introduced. This is done, as depicted in Figure 1 by writing the displacement field $u(\mathbf{x},t)$ as the sum of a continuous displacement $\bar{u}(\mathbf{x},t)$ – the in the absence of strong discontinuity – and of displacement jumps $\bar{\bar{u}}_i(t)$ in sections Γ_i of the solid domain Ω :

$$u(\mathbf{x},t) = \bar{u}(\mathbf{x},t) + \sum_{i=1}^{n_{dis}} \bar{\bar{u}}_i(t)\mathcal{H}_{\Gamma_i}(\mathbf{x}) \tag{1}$$

where $\mathcal{H}_{\Gamma_i}(\mathbf{x})$ is the Heaviside's function which, for a left-to-right oriented domain, is null on the left side of the discontinuity Γ_i and unity on its right side.

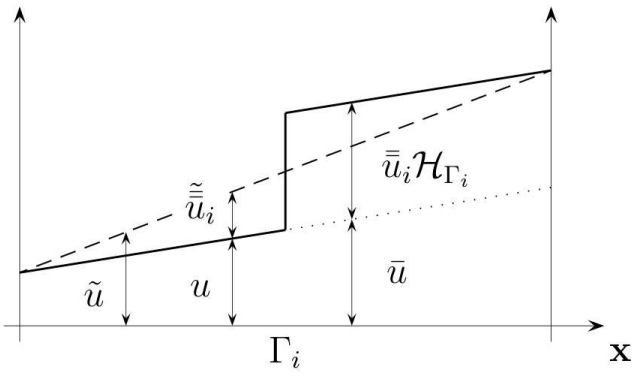

Figure 1: Construction of an enhanced displacement field $u(\mathbf{x},t)$ as the sum of a continuous displacement $\bar{u}(\mathbf{x},t)$ and of a displacement jump $\bar{\bar{u}}_i(t)\mathcal{H}_{\Gamma_i}(\mathbf{x})$ pertaining to discontinuity Γ_i.

The hypothesis of small transformation leads to the following expression for the normal strain field:

$$\epsilon_{xx}(\bar{u},\bar{\bar{u}}_i,t) = \frac{\partial \bar{u}(\mathbf{x},t)}{\partial \mathbf{x}} + \sum_{i=1}^{n_{dis}} \bar{\bar{u}}_i(t)\delta_{\Gamma_i}(\mathbf{x}) \tag{2}$$

where $\delta_{\Gamma_i}(\mathbf{x})$ is the Dirac's function.

2.2. Stored energy function

To derive the governing equations of the system, one can appeal to the principle of minimum potential energy at equilibrium. We write the internal potential energy U^{int} as:

$$\begin{aligned} U^{int}(\bar{u}, \boldsymbol{\alpha}, t) &= \int_{\Omega} \psi\left(\bar{u}, \boldsymbol{\alpha}, t\right) d\Omega \\ &= \sum_{f=1}^{n^c_{fib}} \int_{\Omega^c_f} \psi^c\left(\bar{u}, \boldsymbol{\alpha}^c, t\right) d\Omega^c_f + \sum_{f=1}^{n^s_{fib}} \int_{\Omega^s_f} \psi^s\left(\bar{u}, \boldsymbol{\alpha}^s, t\right) d\Omega^s_f \end{aligned} \tag{3}$$

where $n^{c,s}_{fib}$ is the total number of concrete or steel fibers, $\Omega^{c,s}_f$ is the volume of the fiber, $\psi^{c,s}$ is the stored energy function for concrete or steel which depends on the continuous displacement field $\bar{u}(\mathbf{x}, t)$ and on the set of internal variables $\boldsymbol{\alpha}^{c,s}$. Normal stresses are computed from these functions as

$$\sigma_{xx} = \frac{\partial \psi}{\partial \epsilon_{xx}}. \tag{4}$$

2.3. Set of internal variables

The set of internal variables $\boldsymbol{\alpha}$ is defined to characterize the evolution of the main energy dissipative – inelastic – mechanisms which develop in the system. These internal variables are the memory of the system. The displacement jumps $\bar{\bar{u}}_i$ are treated as internal variables. Note that the constitutive law used here can handle different behavior in compression and tension, and can also reproduce a visco-elastic response (see (Jehel et al. 2010) for a full description). Viscosity is not considered in this work. The local admissible state of the system is expressed according to criteria functions in the stress-like domain of the set of variables dual to $\boldsymbol{\alpha}$. When irreversible mechanisms are activated in the structure, internal variables have to be updated and their evolution is governed by the principle of maximum dissipation. From the computational point of view, because we only consider linear hardening and softening laws, there is no need for local iteration when internal variables are updated, except for transitions between hardening and softening regimes, which leads to an efficient resolution procedure. Figure 2 illustrates the capabilities of such an uniaxial constitutive law with linear hardenings / softenings for representing the cyclic compressive behavior of concrete.

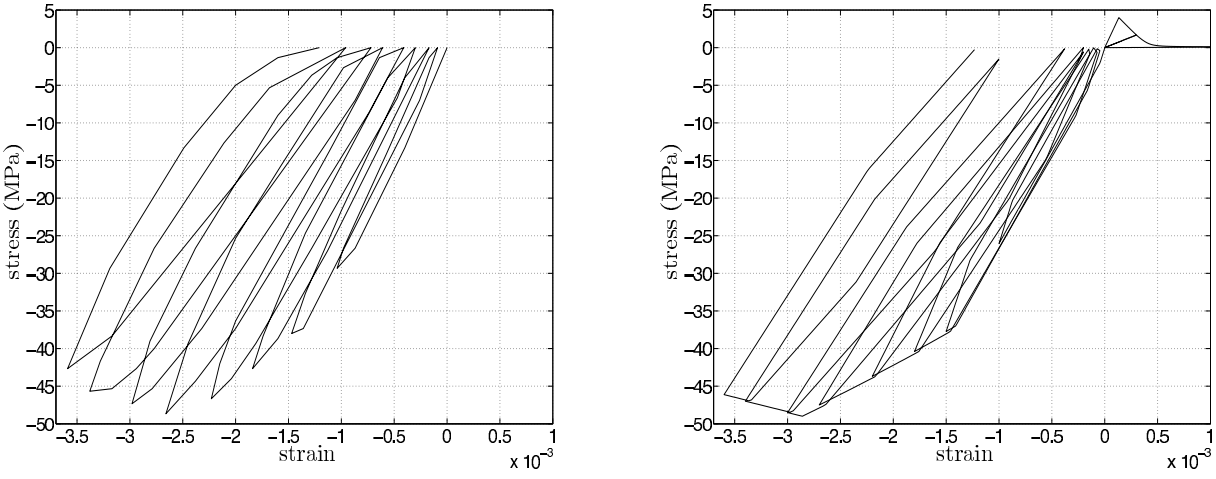

Figure 2: [left] Experimental response of concrete in cyclic compressive loading (Ramtani 1990); [right] Numerical constitutive law used in this paper.

3. CONSISTENT ADDITIONAL DAMPING MODEL

3.1. Problems encountered with Rayleigh damping

Controlling the amount of additional viscous damping energy dissipated in inelastic time history analyses is a very challenging task (Léger & Dussault 1992, Hall 2006, Charney 2008). This is especially the case for commonly used Rayleigh proportional damping models, that is when the damping matrix is computed, in its most general form, as

$$\mathbf{C}(t) = \alpha(t)\mathbf{M} + \beta(t)\mathbf{K}(t), \tag{5}$$

where $\mathbf{K}(t)$ is the tangent stiffness matrix. Several researchers have provided insight in the comprehension of Rayleigh damping regarding the inelastic structural model it is coupled to, have highlighted limitations, and have eventually provided recommendations to cope with them (Léger & Dussault 1992, Hall 2006, Charney 2008). Nevertheless, adding damping and controlling its consistency with the inelastic structural model still remains an issue to be addressed.

3.2. Three common phases in seismic response

We now discuss in a qualitative way the notion of *consistency* for additional viscous damping. To that purpose, we start by stating that seismic structural response is composed by three main consecutive phases, as illustrated in Figure 3. Both inelastic structural model and additional damping model must then be capable of representing the salient phenomena corresponding to each of these three phases. Foremost has to be properly modeled what we call here the "key window", namely the time interval within which the major inelastic modifications for structural performance assessment develop. For instance, key mechanisms that control near-collapse structural behavior are listed in (Krawinkler 2006): degradation of strength and stiffness, and structure P-delta effects. From experimental results, we know that strain rate is another major issue.

A consistent additional damping model should be adapted to each of these three phases as follows:

- Phase 1: None or only few incursions in the inelastic domain occur. Energy dissipation in phase 1 thus comes from the friction in the cracks that appeared when applying dead load and from other mechanisms always present in mechanical systems. When used, visco-elasticity and constitutive laws with local hysteresis (Ragueneau et al. 2000, Jehel et al. 2010) in the structural model could account for these energy dissipation sources but a small amount of additional damping usually has to be added.

- Phase 2: As the ground motion becomes stronger (at around $8s$ in Figure 3), an important amount of seismic energy is imparted to the structure and some parts of the structure then exhibit inelastic behavior. Inelastic structural models are designed to explicitly model part of the numerous inherent nonlinear energy dissipative mechanisms involved in the structural response. The energy dissipation due to the mechanisms not explicitly accounted for in the inelastic structural model has to be introduced with the additional damping model.

- Phase 3: The structure has suffered irreversible degradations that modified its dynamic properties. Thus, even if the seismic demand is again as low as in phase 1, the energy dissipative mechanisms are different because of frictions in the cracks that appeared within phase 2 or at degraded bound between steel and concrete. Here again, visco-elasticity and behavior laws with local hysteresis (Ragueneau et al. 2000, Jehel et al. 2010) in the structural model could account for these damping sources, but it generally has to be completed by additional damping.

3.3. Proposition of a new family of Rayleigh damping models

In the following, two damping models will be used:

- A commonly used Rayleigh model based on tangent stiffness matrix and with two constant coefficients

$$\mathbf{C}_1(t) = \alpha\mathbf{M} + \beta\mathbf{K}(t); \tag{6}$$

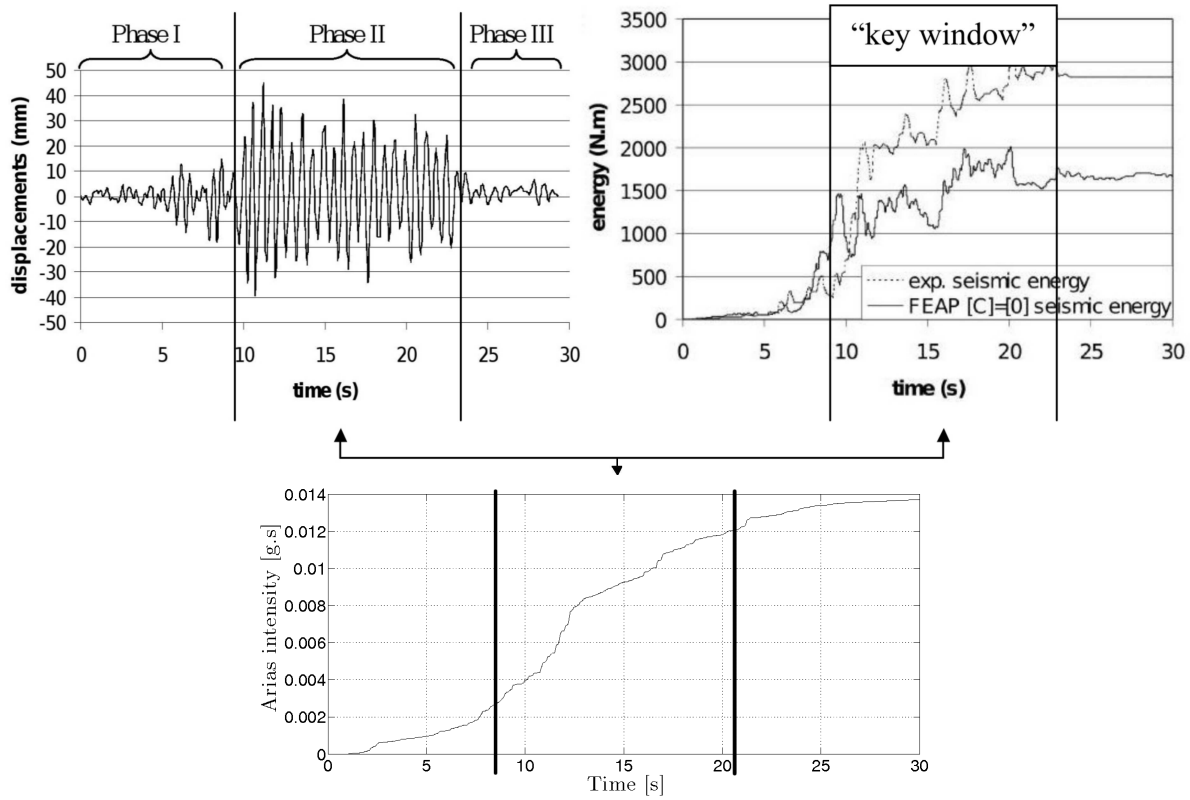

Figure 3: Three common phases in the seismic response and the concept of "key window". [top left] Structural relative displacement time-history. [top right] Total relative seismic energy time-history in the structure. [bottom] Arias intensity of the seismic signal that will be used in the following numerical simulations: $AI(t) = \frac{\pi}{2g}\int_0^t \ddot{u}_g^2(\tau)d\tau$ (Arias 1970).

- We propose a model that is dependent on both the two key notions in the definition of the three phases introduced above: the capacity of the inelastic structural model to absorb energy and the seismic demand. The model is based on Rayleigh damping with tangent stiffness matrix and with coefficients adapted to each of the three phases:

$$\mathbf{C}_2(t) = \alpha(t)\mathbf{M} + \beta(t)\mathbf{K}(t) \tag{7}$$

The idea of adapting Rayleigh damping to the capabilities of the inelastic structural model for dissipating energy is present in the use of the tangent stiffness rather than the initial one: it is expected that the choice of tangent stiffness dependent damping will have the main advantage of providing the significant additional source of damping only in the domains/modes that are not accounted for by inelastic model. Such a choice allows to provide the physically based damping phenomena interpretation, which leads to damping coefficients that are easier to identify. The same idea has been further exploited in (Tinawi et al. 2000) where 1% viscous damping is added to an inelastic dam model before cracking and 10% after cracking to represent localized high dissipation by friction between crack lips.

In spite of its stronger physical background, implementing damping model $\mathbf{C}_2(t)$ is not as straightforward as damping model $\mathbf{C}_1(t)$. First, three sets of Rayleigh coefficients $(\alpha_p, \beta_p)_{p=1,2,3}$ corresponding to each of the three phases p have to be identified to define the critical damping ratio ξ. Second, the instants which delimit the three phases have to be determined, which can be automatically accomplished by the computer program that is capable of detecting the activation of significant inelastic behavior.

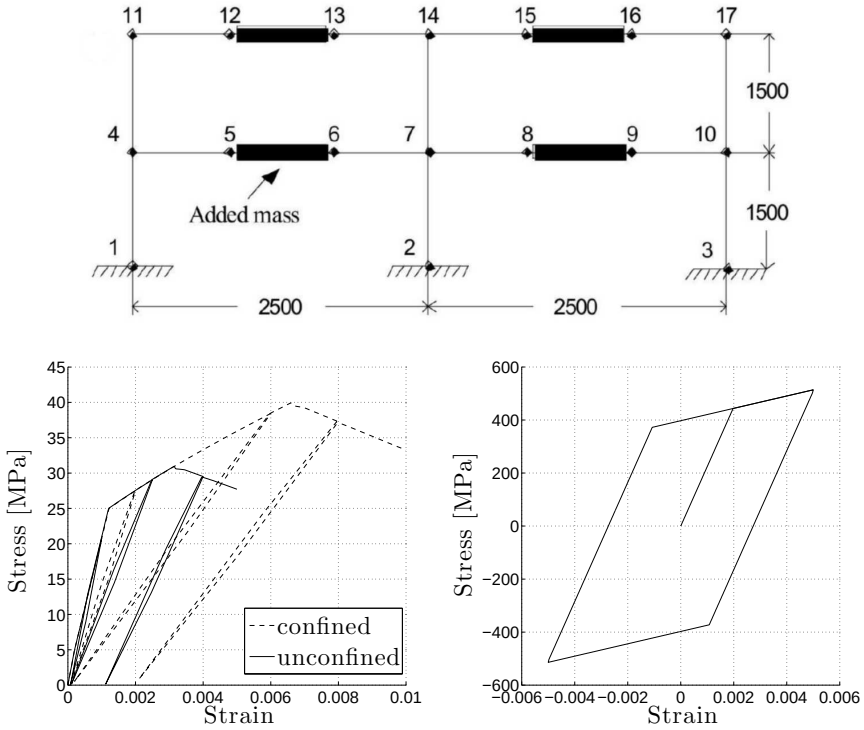

Figure 4: Finite element mesh (dimensions in [mm]) and material constitutive laws for the inelastic structural modeling. The black rectangles represent additional masses. [bottom left] Confined and unconfined concrete behavior laws. [bottom right] Steel constitutive law.

4. NUMERICAL SIMULATIONS

Seismic inelastic time history analyses of the RC frame shown in Figure 4 have been carried out with the inelastic structural model briefly presented in section 2 coupled to either additional damping model $\mathbf{C}_1(t)$ or $\mathbf{C}_2(t)$. The implicit Newmark integration scheme with parameters $\beta = 0.25$ and $\gamma = 0.5$ is used with a time step of $0.005s$. The elastic fundamental period of the structure is $T_0 = 0.28s$. The ground motion record that was selected for the test program corresponds to the N04W component of the accelerogram recorded in Olympia, Washington (April 13, 1949), calibrated to a peak ground acceleration $PGA = 0.21g$. Figure 5 shows a comparison between the simulated top-displacement and energies time histories and the respective experimental results reproduced from (Filiatrault et al. 1998b). Good agreement between simulated and experimental data can be observed. Moreover, there is very good agreement between the hysteretic (E_H) and damping (E_D) energy quantities computed with the models proposed here and an analogous Perform3D (Perform3D 2000) simulation we carried out for comparison purpose, namely $E_H \approx 550N.m$ and $E_D \approx 2250N.m$, corresponding to approximately 20% and 80% of the total work done by the structure during seismic motions.

For damping model $\mathbf{C}_1(t)$, the good results shown in Figure 5 have been obtained with α and β computed so that damping ratios $\xi_1 = \xi_2 = 3.3\%$. For damping model $\mathbf{C}_2(t)$, curves plotted in Figure 5 have been obtained with the following parameters identified so as to obtain good match between experimental and simulated responses:

- Phase 1: from $0 \leq t \leq t_1$, $\xi_1 = \xi_2 = 1.0\%$. We set $t_1 = 8s$ because it corresponds to the time when the seismic demand – evaluated here through the Arias intensity $AI(t)$ of the ground motion, which is plotted in Figure 3 [bottom] – starts to significantly increase. Because of the application of additional masses before the ground motion, the structure is initially damaged so, even if the structural model is capable of reproducing the main energy dissipation mechanisms, we assume a small amount of additional damping has to be introduced.
- Phase 2: from $t_1 \leq t \leq t_2$, $\xi_1 = \xi_2 = 4.0\%$. t_2 is heuristically defined as $t_2 = t_1 + 10 \times T_1^{ini}$,

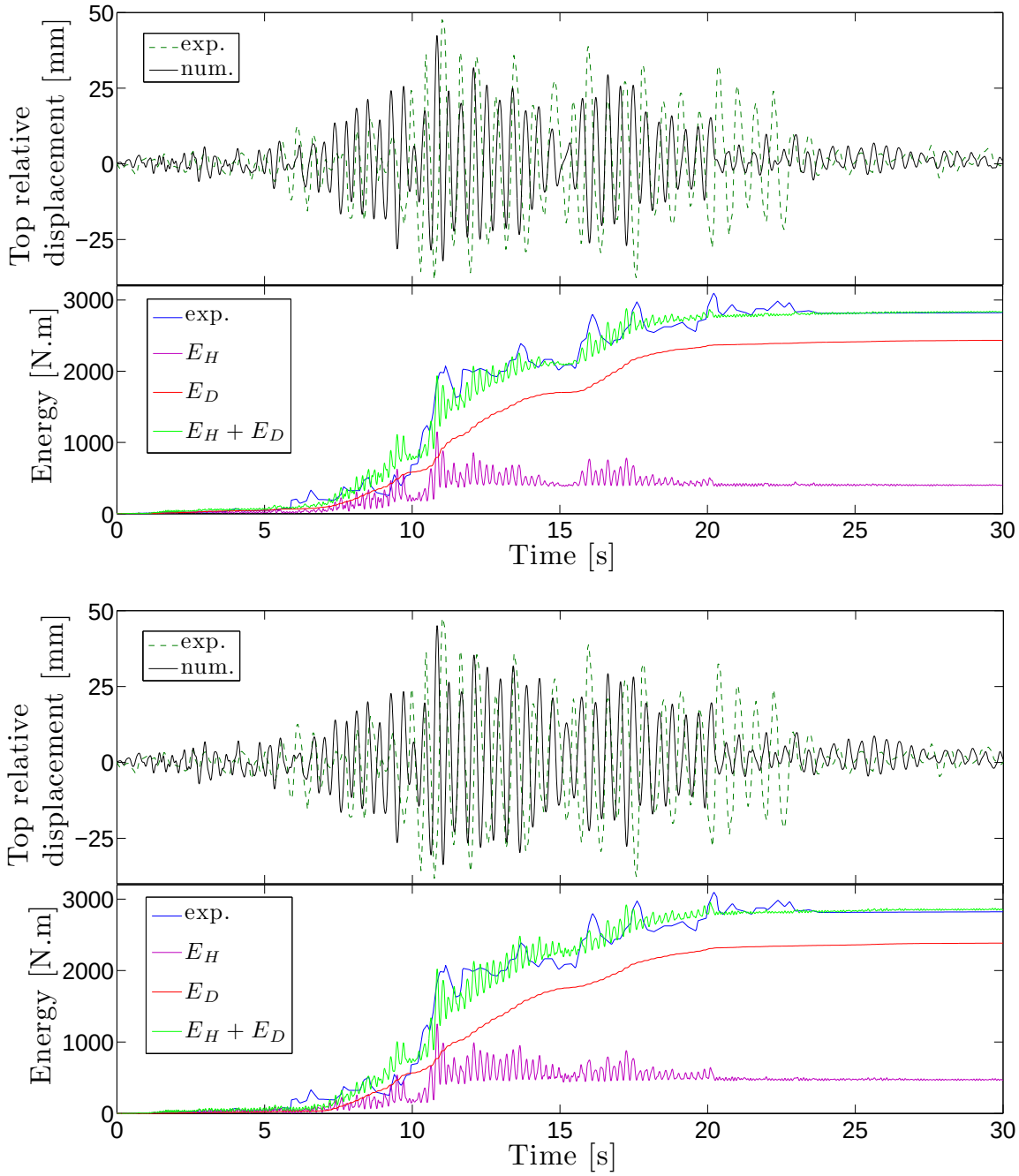

Figure 5: Experimental and simulated top-displacement; simulated hysteretic energy (E_H), simulated additional damping energy (E_D), and both experimental and simulated total internal work. [top] With common added damping model $\mathbf{C}_1(t)$; [bottom] With the proposed Rayleigh damping model $\mathbf{C}_2(t)$. The structural responses shown here for damping models $\mathbf{C}_1(t)$ and $\mathbf{C}_2(t)$ looks very similar because both models have been calibrated to experimental data; however, model $\mathbf{C}_2(t)$ has more capability for representing transient evolution of added damping.

where T_1^{ini} is the fundamental period of the structure after dead load has been applied and just before the ground motion ($T_1^{ini} = 0.36s$ for the structure considered here). t_2 is identified so as to recover good fit between both experimental and numerical total energy dissipation curves. ξ_1 and ξ_2 are set to 4% because cracks in the beam-to-column joints have been experimentally observed and the structural model is not capable of representing such mechanisms, so the damping ratio is increased comparing to phase 1.

- Phase 3: from $t_2 \leq t \leq \bar{T}$, $\xi_1 = \xi_2 = 2.5\%$, where $\bar{T}$ is the duration of the seismic signal. The damping ratio is decreased but to a higher level than in phase 1 because the damage structure exhibit more energy dissipation mechanisms (cracks, plastic hinges).

Both additional damping models $\mathbf{C}_1(t)$ and $\mathbf{C}_2(t)$ lead to very close results in Figure 5. Besides, damping model $\mathbf{C}_2(t)$ is designed to be consistent with both the capacity of the structural model to dissipate energy and the seismic demand. Consequently, one can infer that both additional damping models $\mathbf{C}_1(t)$ and $\mathbf{C}_2(t)$ are consistent, even if they dissipate much more energy than the inelastic structural model. Of course, damage in the beam-to-column joints is not predicted, but the inelastic evolution of the beams and columns should be quite well reproduced, which should be assessed by further comparison with experimental data.

5. CONCLUSIONS

In this paper, an additional damping model consistent with both the capability of the inelastic structural model to dissipate seismic energy and the seismic demand is presented and the simulation of a 2D RC frame tested on a shaking table is performed with this latter damping model. These numerical results, along with experimental data, are then used as a baseline to assess the consistency of another more common Rayleigh damping model. The consistent damping model relies on the definition of three successive phases in the typical seismic response of RC frames, corresponding to different seismic demand levels and to the capability of the inelastic structural model to dissipate seismic energy.

The structural model used in this work is a fiber beam/column model with material constitutive laws capable of representing the main energy dissipation mechanisms in concrete and steel. However, it cannot reproduce structural inelastic phenomena such as inelastic beam-to-column joints behavior, rebar slip, steel buckling, or energy radiation. Thus, developing structural models describing these latter mechanisms is to be continued so as to provide efficient numerical tools capable of predicting the structural response in an even more accurate way.

ACKNOWLEDGEMENT

The authors thank Pr. André Filiatrault for providing the data from the shaking table tests used in this work.

REFERENCES

Arias, A. (1970) Seismic Design for Nuclear Power Plants, *A measure of earthquake intensity*, pp. 438–483. MIT Press, Cambridge, MA.

Charney, F.A. (2008). Unintended consequences of modeling damping in structures. *Journal of Structural Engineering* **134:4**, 581–592.

FEAP: A Finite Element Analysis Program, User Manual and Programmer Manual, version 7.4. (October 2002). Department of Civil and Environmental Engineering, University of California, Berkeley, CA.

Filiatrault, A., Lachapelle, E. and Lamontagne, P. (1998). Seismic performance of ductile and nominally ductile reinforced concrete moment resisting frames – I. Experimental study. *Canadian Journal of Civil Engineering* **25** 331–341.

Filiatrault, A., Lachapelle, E. and Lamontagne, P. (1998). Seismic performance of ductile and nominally ductile reinforced concrete moment resisting frames – II. Analytical study. *Canadian Journal of Civil Engineering* **25**, 342–351.

Garikipati, K. and Hughes, T.J.R. (1998). A study of strain localization in a multiple scale framework – the one-dimensional problem. *Computational Methods in Applied Mechanics and Engineering* **159**, 193–222.

Germain, P., Nguyen, Q.S. and Suquet, P. (1983). Continuum thermodynamics. *Journal of Applied Mechanics* **50**, 1010–1020.

Hall, J.F. (2006). Problems encountered from the use (or misuse) of Rayleigh damping. *Earthquake Engineering and Structural Dynamics* **35**, 525–545.

Ibrahimbegovic, A. and Brancherie, D. (2003). Combined hardening and softening constitutive model of plasticity: precursor to shear slip line failure. *Computational Mechanics* **31**, 89–100.

Jehel, P., Ibrahimbegovic, A., Léger, P., Davenne, L. (2010). Towards robust viscoelastic-plastic-damage material model with different hardenings / softenings capable of representing salient phenomena in seismic loading applications. *Computers and Concrete* **7:4**, 365–386.

Krawinkler, H. (2006) Importance of good nonlinear analysis. *The structural design of tall and special buildings* **15**, 515–53.

Léger, P. and Dussault, S. (1992). Seismic-Energy Dissipation in MDOF Structures. *ASCE Journal of Structural Engineering* **118:6**, 1251–1267.

Maugin, G.A. (1999). The thermodynamics of nonlinear irreversible behaviors – An introduction. World Scientific, Singapore.

Oliver, J. and Huespe, A.E. (2004). Theoretical and computational issues in modeling material failure in strong discontinuity scenarios. *Computer Methods in Applied Mechanics and Engineering* **193**, 2987–3014.

PEER/ATC-72-1 (October 2010). Modeling and Acceptance Criteria for Seismic Design and Analysis of Tall Buildings, prepared by Applied Technology Council for Pacific Earthquake Engineering Research Center.

CSI (2007). Perform3D User's manual. Technical report, California.

Ragueneau, F., La Borderie, C. and Mazars, J. (2000). Damage model for concrete-like materials coupling cracking and friction, contribution towards struc-ural damping: first uniaxial applications. *Mechanics of Cohesive-Frictional Materials* **5**, 607–625.

Ramtani, S. (1990). Contribution to the modeling of the multi-axial behavior of damaged concrete with description of the unilateral characteristics. PhD thesis (in French): Paris 6 University.

Tinawi, R., Léger, P., Leclerc, M. and Cipolla, G. (2000) Seismic safety of gravity dams: from shake table experiments to numerical analyses. *ASCE Journal of Structural Engineering* **126:4**, 518–529.

Zareian, F. and Medina, R.A. (2010). A practical method for proper modeling of structural damping in inelastic plane structural systems. *Computers and Structures* **88**, 45–53.